Dynamic Glass Transition of the Rigid Amorphous Fraction in Polyurethane-urea/SiO_2 Nanocomposites

Stefanos Koutsoumpis, Konstantinos N. Raftopoulos, Oguzhan Oguz, Christine M. Papadakis, Yusuf Menceloglu and Polycarpos Pissis

Supporting Information

Equations for the analysis of DRS spectra

The relaxations are evident as peaks in the dielectric loss ε'' spectra, which can be described using the Havriliak-Negami (H-N) function:[1]

$$\varepsilon''(f) = Im[\frac{\Delta\varepsilon}{[1+(if/f_{HN})^a]^b}]$$

where f_{HN} is a characteristic frequency related to the frequency of maximum loss (f_{max}), $\Delta\varepsilon$ is the relaxation strength and *a* and *b* are shape parameters. The temperature dependence of the time scale of the dielectric response can be followed through the Arrhenius plot (activation diagram, plot of the logarithm of the frequency of the dielectric loss peak against reciprocal temperature) and be further analyzed by fitting appropriate equations. The Arrhenius equation is common for describing local dynamics:[2]

$$f_{max}(T) = f_0 exp\left(-\frac{E_{act}}{kT}\right)$$

where f_{max} is the frequency of ε''(f) peak, T the temperature, f_0 a pre-exponential constant, E_{act} the activation energy of the relaxation and k Boltzmann's constant. The Vogel-Tammann-Fulcher equation (VTF) equation, characteristic of cooperative processes, was used to describe the time scale dependence on temperature:[2]

$$f_{max}(T) = f_0 e^{-\frac{B}{T - T_0}}$$

where *B* is the apparent activation energy, f_0 the pre-exponential frequency factor and T_0 the Vogel temperature. The strength parameter was calculated as $D=B/T_0$ and the fragility as $m=16+590/D$.[3]

In order to extract information for relaxations masked by DC conductivity the derivative formalism was used. The frequency derivative of ε' contains the same information on polarization effects as ε'' but excludes the effect of σ_{dc}:[4,5]

$$\varepsilon''_{der} = -\frac{\pi \partial \varepsilon'(\omega)}{2\, \partial\, ln\omega}$$

Supplementary Figures and text

In Supporting Figure 1 we present the cooling DSC thermograms for the TPU 4k samples. The lower crystallization temperature suggests slower crystallization kinetics.[6] From the area of the peaks we calculate the crystallinity – Crystalline Fraction.

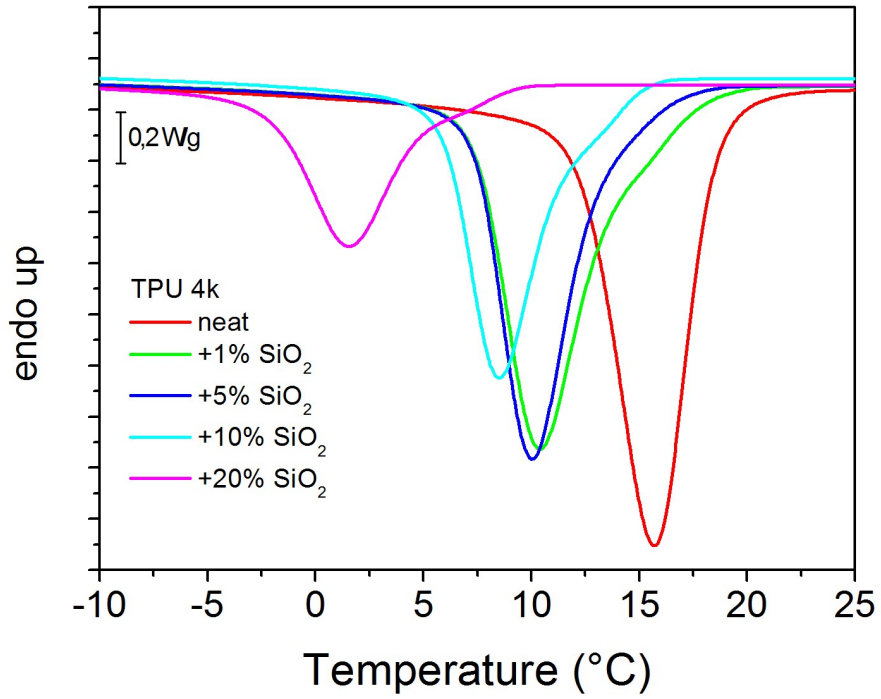

Supporting Figure 1 DSC Thermograms during cooling from melt at 10 °C/min, focused on the crystallization temperature region for the samples TPU 4k

Heating DSC thermograms for the three matrices are presented in Supporting Figure 2. The TPU 2k, fully amorphous at low temperature, displays a large glass transition step, a cold-crystallization peak and a melting peak, whereas the other matrices crystallized during cooling and display a small glass transition step and a melting peak. The increasing melting temperature suggests better/more perfect crystals.[6]

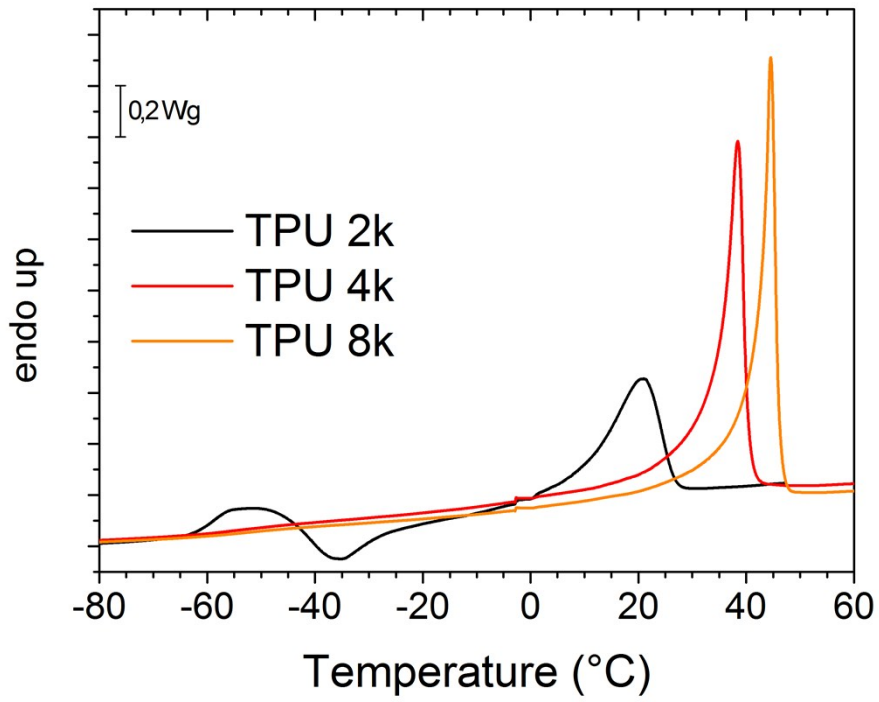

Supporting Figure 2 Heating thermograms for the three matrices. The melting temperature increases with increasing M_W of the soft segments.

In Supporting Figure 3 results of calculations for MAF and RAF vs. filler content for the samples TPU 4k can be found.

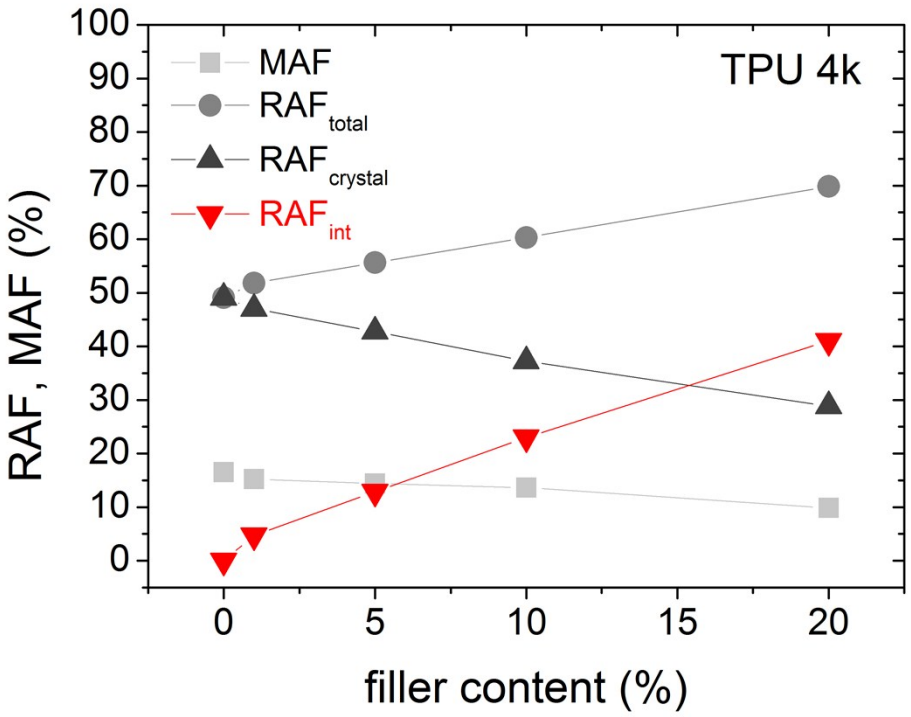

Supporting Figure 3 Values for MAF, RAF, $RAF_{crystal}$ and RAF_{int} in the TPU 4k samples vs. filler content. The lines connencting the experimental points are used as guides for the eye.

At low temperatures we follow two local molecular motions: β-relaxation at low frequencies and γ-relaxation at high frequencies (Supporting Figure 4). The relaxations appear as peaks in the diagrams of dielectric losses ε'' vs. frequency. The γ-relaxation has been associated with local motion of $(CH_2)_n$ sequences[7] and the β-relaxation with the reorientation of polar carbonyl groups with attached water molecules.[8] No effect of the filler or the M_W of the soft segments on the relaxation time was observed. The activation energy for the relaxation was computed by fitting the Arrhenius equation (Supporting Figure 5) to the data. The activation energy and the pre-exponential parameters computed are $E_{act,\gamma}$ = 0,38 eV, log $f_{0,\gamma}$ = 14.4, $E_{act,\beta}$ = 0,67 eV, log $f_{0,\beta}$ = 18.1. The activation energy for β-relaxation is almost double as compared to that of γ, even though the relaxations show similar time scales. This is counterbalanced by the high value of f_0 for the β-relaxation. The parameter f_0 is related with lattice vibrations. Since the value derived from the fitting is unreasonably high for the β-relaxation, and by taking into account that the Arrhenius equation is a phenomenological one, it is most probable that there is a percentage of cooperativity in this relaxation.[9]

The γ-relaxation has similar activation energy with that reported in previous work by Kanapitsas et al.[7], Koutsoumpis et al.[10] (E_{act}= 0.34, log f_0=14.7), and Raftopoulos et al.[11] (E_{act} = 0.39 eV, log f_0=15.4). The activation parameters of the β-relaxation show a scattering in the literature,[7,10,11] most probably reflecting different hydration levels of the samples studied.

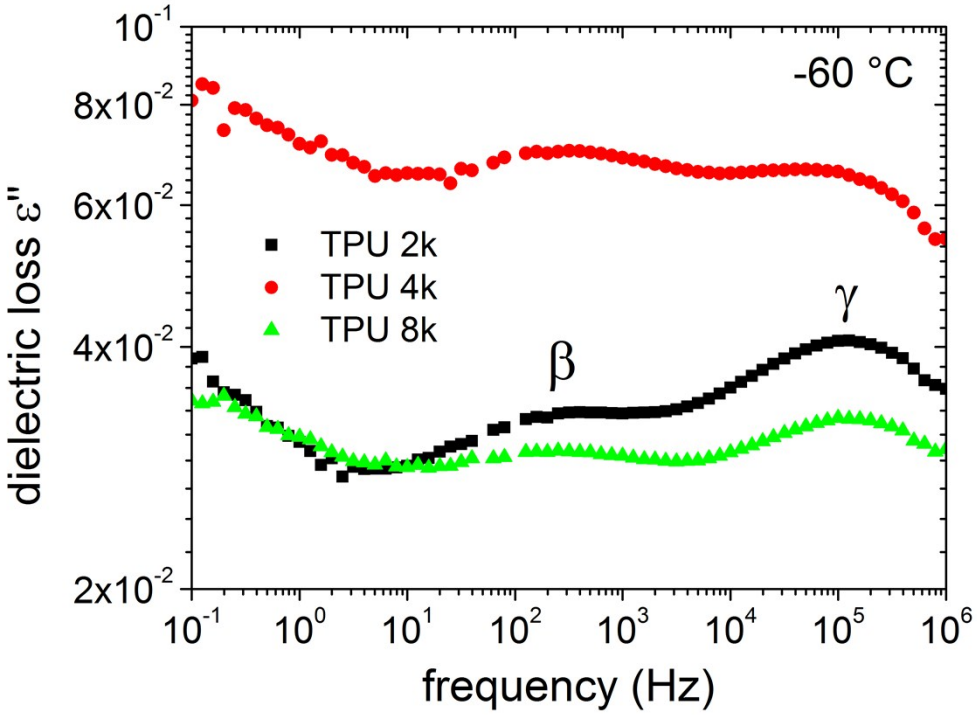

Supporting Figure 4 DRS spectra for the three matrices at -60 °C, where the β and γ relaxations are in the frequency window of measurements

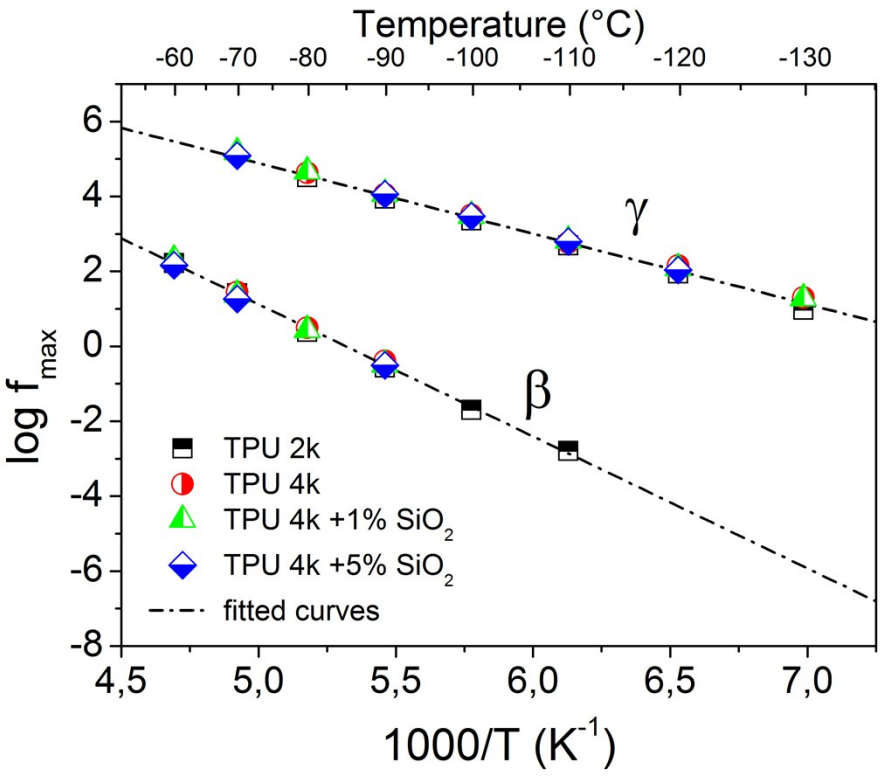

Supporting Figure 5 Arrhenius plot for the β and γ relaxations for the samples noted in the graph. The lines are fittings of the Arrhenius equation to the experimental data.

The α-relaxation (dynamic glass transition) is expected to be observed as a peak in the diagrams of ε′′ vs. frequency (isothermal measurements) at temperatures higher than T_g.[12] What we observe is a "jump" for the values of ε′′ above T_g due to an overall increase of the conductivity of the system, but no peak for the α-relaxation (Supporting Figure 6). As the temperature increases, the peaks of β and γ relaxations are still visible, shifting to higher frequencies and merging at high temperatures.

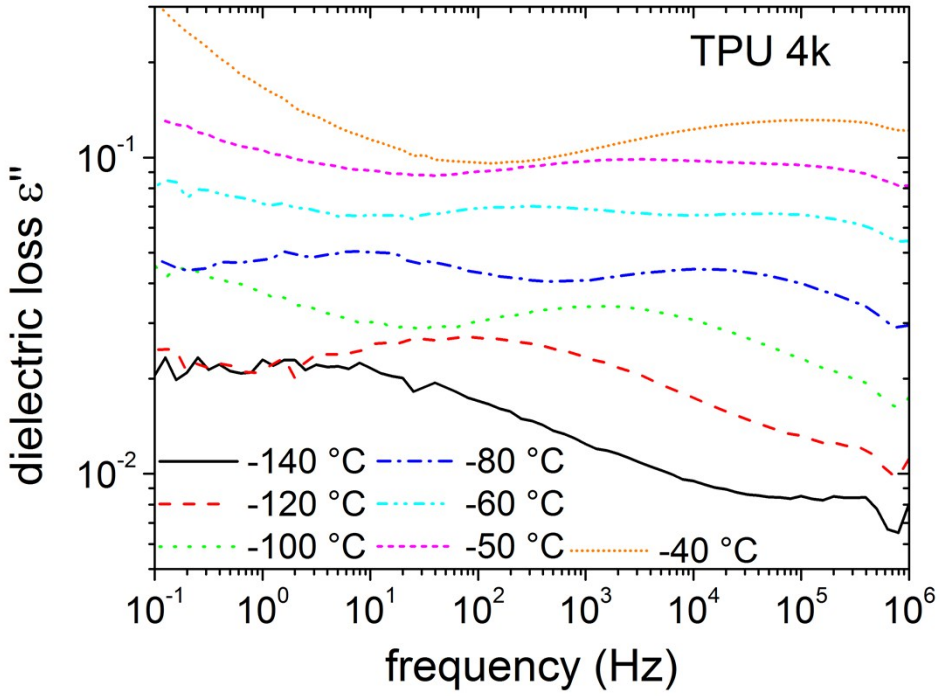

Supporting Figure 6 Dielectric loss spectra for TPU 4k in the temperature range -140 °C to -40 °C

The fitting parameters of the VTF equation for the α-relaxation (Figure 5 of the main text) are found in Supporting Table 1. After a first fitting with all the parameters free, log f_0 was fixed to the mean value for all the samples of each series and a second fitting was done.

Supporting Table 1 Fitting parameters of the VTF equation for the α-relaxation (Figure 5 of the main text) in all the samples studied

Sample	logf_0	B (K)	T_0 (K)	T_g (°C)	D
TPU 2k	9.3	324	207	-55.0	1.6
TPU 4k	10	452	204	-54.1	2.2
TPU 4k +1% SiO_2	10	447	204	-54.0	2.2
TPU 4k +5% SiO_2	10	471	203	-54.0	2.3
TPU 4k +10% SiO_2	10	452	208	-49.5	2.2
TPU 4k +20% SiO_2	10	513	211	-44.3	2.4
TPU 8k	10.8	463	206	-52.7	2.2
TPU 8k +10% SiO_2	10.8	627	207	-46.3	3.0

Conductivity Relaxation and Maxwell-Wagner-Sillars polarization

At higher temperatures, effects of conductivity dominate the dielectric spectra and polarizations related to microphase separation and conductivity relaxations are observed. The analysis by dielectric spectroscopy in this system is quite challenging due to the high conductivity of PEO. Nevertheless, proper analysis of the data will provide additional information on microphase separation and on effects of filler on molecular mobility. In order to approach better the results, we compare diagrams of different quantities obtained using various formalisms, such as ε′ and ε′′, their ratio tanδ, the real part of complex conductivity σ'_{AC}, the imaginary part of the electric modulus M′′, and the frequency derivative of ε′.[4,5] Comparison of these diagrams enables to attribute different features observed to different phenomena (electrode polarization, conductivity relaxation etc.).[5] We compared such diagrams at temperatures from -60 up to 20 °C for all the samples referred in this study.

As an example, such a plot is presented in Supporting Figure 7 for TPU 8k at 25 °C. Two polarizations are observed in this plot, one at ca. 1 Hz and one at ca. 1 kHz. In the spectra of ε′, they appear as "shoulders". Similarly, two shoulders are observed in the spectra of σ'_{AC}. In the spectra of ε′′ and the derivative of ε′ they are apparent as peaks, partly hidden under a strong background related to high conductivity. In M′′ and tanδ, they are apparent as peaks again.

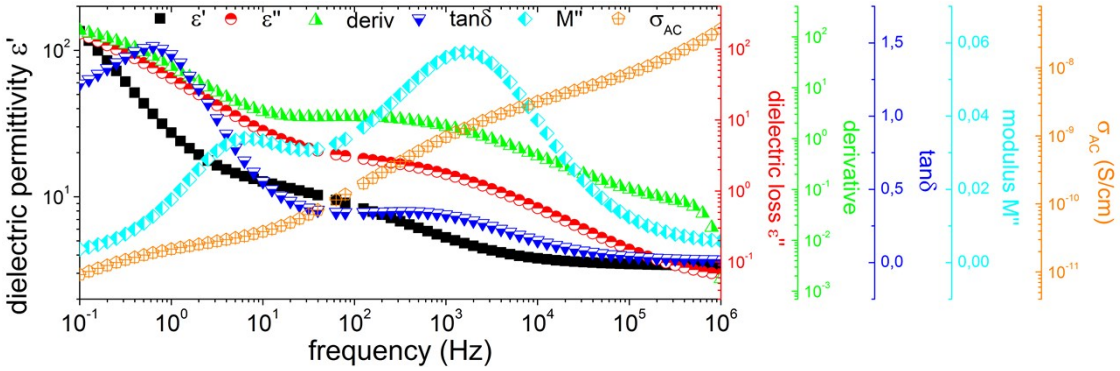

Supporting Figure 7 Comparative plot for various formalisms (ε′,ε′′, σ′$_{AC}$, M′′, derivative, tanδ) for TPU 8k matrix at 25 °C

Comparison of the different formalisms helps to clarify the origin of these two polarizations. The frequency derivative of ε′ (the equation used for that is given in the supporting information) results in curves similar to ε′′ without the contribution of dc-conductivity,[4] but not much information could be obtained from that: the phenomena that hide the peaks of ε′′ are rather not dc-conductivity but most probably polarization of space charges, such as Maxwell-Wagner-Sillars (MWS) polarization,[5,8] electrode polarization,[13] or conductivity relaxation.[12,13]

The polarization at ca. 1 Hz is related to conductivity relaxation, the transition from dc to ac conductivity: by comparing the spectra of electric modulus M′′ and conductivity σ′$_{AC}$, we observe that the peak of M′′ is slightly shifted to higher frequencies than the "knee" of the conductivity.[12] The peak at ca. 1 kHz is a MWS polarization/relaxation: in polyurethanes, MWS polarization is known to exist at temperatures higher than T_g and is related to the microphase separation.[8] This interfacial polarization is due to mobility and accumulation of charges in the interface of regions with different conductivity, soft and hard domains of PU-urea in our case, and is typical for inhomogeneous materials.[5]

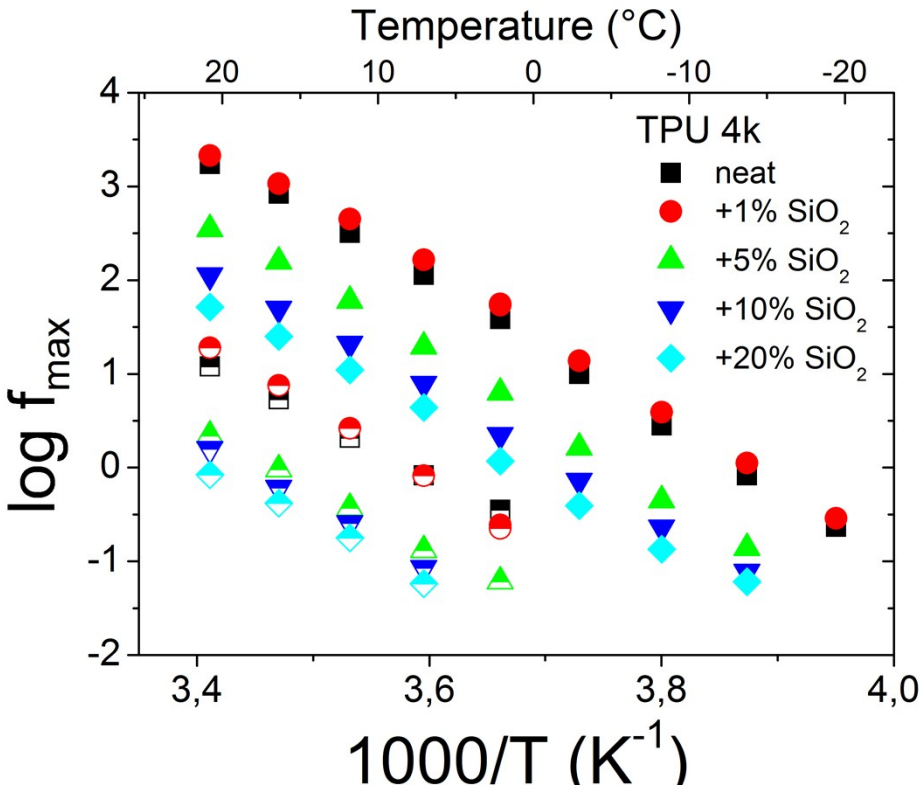

Supporting Figure 8 Arrhenius plots of MWS and conductivity relaxation for the TPU 4k samples. Solid symbols stand for the MWS relaxation, half-filled for the conductivity relaxation.

We construct the Arrhenius diagram for the samples by fitting an equation of the Havriliak-Negami type to the experimental data for the modulus formalism (the two peaks of M'', compare Supporting Figure 7) and focusing on the time scale of the response. In Supporting Figure 8 the Arrhenius plot for the TPU 4k samples is presented, while the Arrhenius plots for the other samples may be found in the Supporting Figures 9 and 10. For the TPU 4k samples, both relaxations become systematically slower by addition of filler. The decreased conductivity is an indirect indication of the existence of RAF_{int}. At this stage, please note that although the position of MWS is related to micromorphology, no safe conclusions can be extracted here because of the complexity of the system and the many phases of different conductivity. We would like to stress though that the activation energy (slope of the Arrhenius trace) of both MWS and conductivity remains mostly unaffected on addition of nanoparticles. This indicating that the mechanism of charge transport remains mostly the same, i.e. carriers moving through the soft phase encounter similar environments, i.e. we

believe that the soft phase does not change significantly consistency, in the sense that the amount of dissolved hard segments is rather unaffected. However, with increasing filler content the slowing down of the relaxations and the decreasing conductivity values may indicate that the “conductive paths” are now fewer or narrower. Such an effect might be caused by nanoparticles with their surrounding uncrystalizable and immobile RAF residing in the soft phase and thus “blocking” the conductive pathways.

The conductivity and the MWS relaxation exhibit VTF shape in the TPU 4k samples, indicating cooperativity. In addition, parallel traces of the two processes for each sample indicate similar activation energies. The pattern of slower relaxations on addition of filler is in agreement with the pattern of decreased conductivity, so both relaxations are strongly correlated to the overall conductivity of the system.

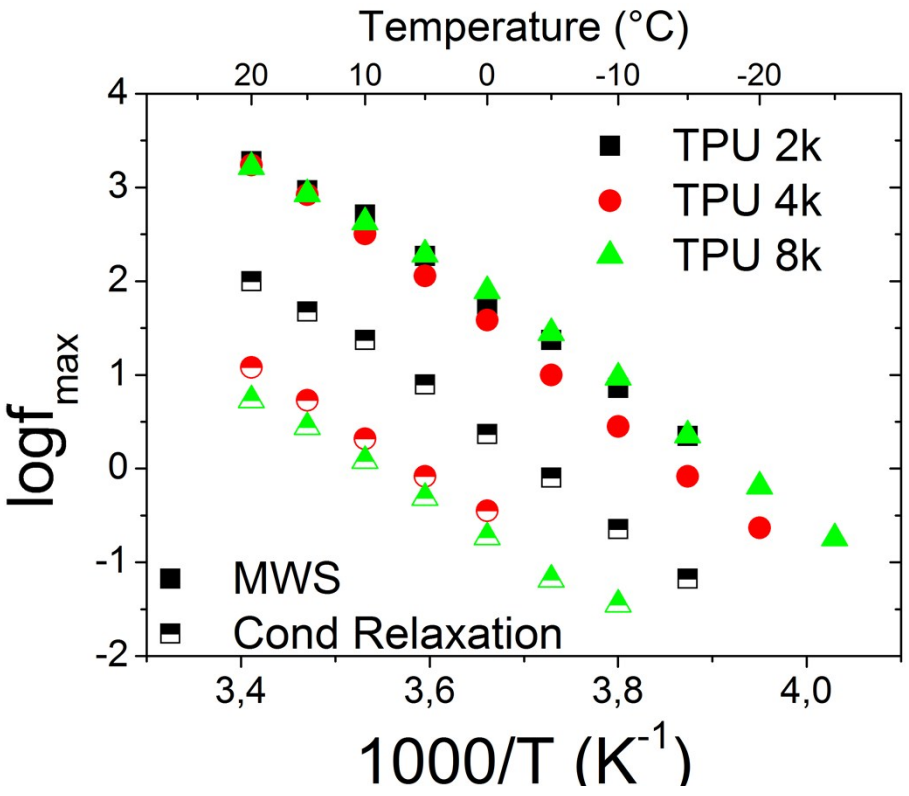

Supporting Figure 9 Arrhenius plots for the MWS and conductivity relaxations for the three neat matrices. Filled symbols stand for the MWS relaxation, half-filled for the Conductivity relaxation.

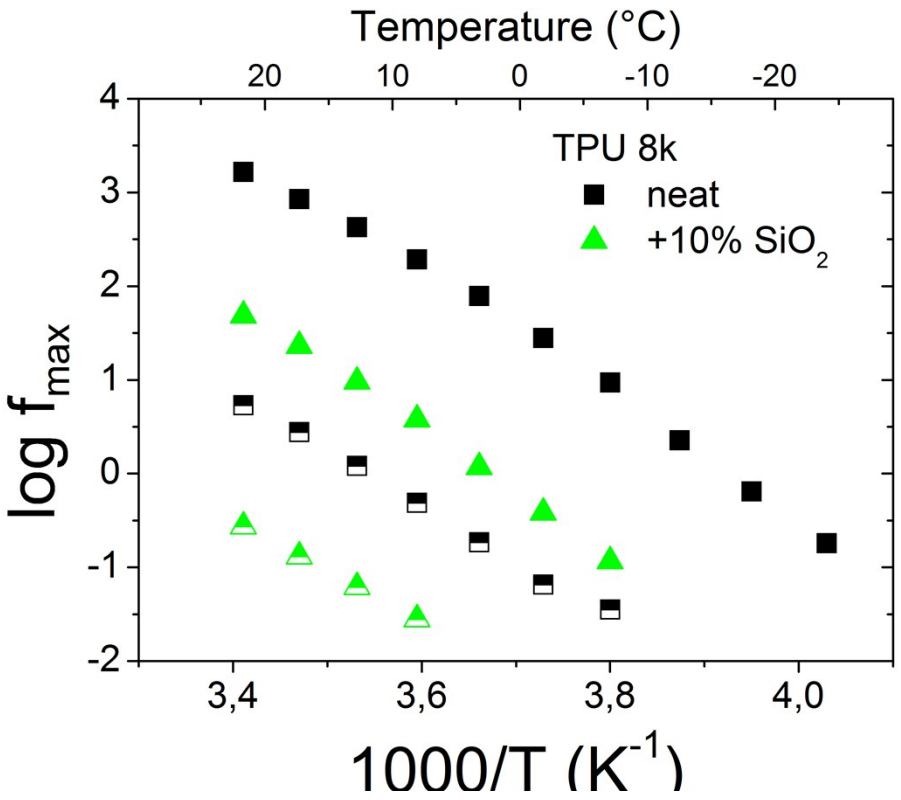

Supporting Figure 10 Arrhenius plots for the MWS and conductivity relaxations for TPU 8k and TPU 8k +10% SiO. Close symbols stand for the MWS relaxation, half-filled for the Conductivity relaxation.

In the X-Ray scattering curves, we observe multiple peaks at wide angles related to crystalline structures. We calculated the crystallinity as the ratio of the area of the peaks and the total area under the curves $X_c = I_{peak}/I_{total}$. This value was then normalized to the soft segment ratio, the same way we did for the calculation of crystallinity by DSC. DSC and SAXS result in similar crystallinities for the samples measured. In Supporting Figure 11 the crystallinity values vs. filler content are presented for the three matrices. The pattern of decreasing crystallinity with increasing filler content is common for all matrices and has been observed before in polymer/silica nanocomposites.[14,15] TPU 4k and TPU 8k display similar values and pattern. In the case of TPU 8k 20wt% SiO2, the increased crystallinity can be attributed to poor filler dispersion. TPU 2k, with the shorter soft segments, displays lower crystallinity.

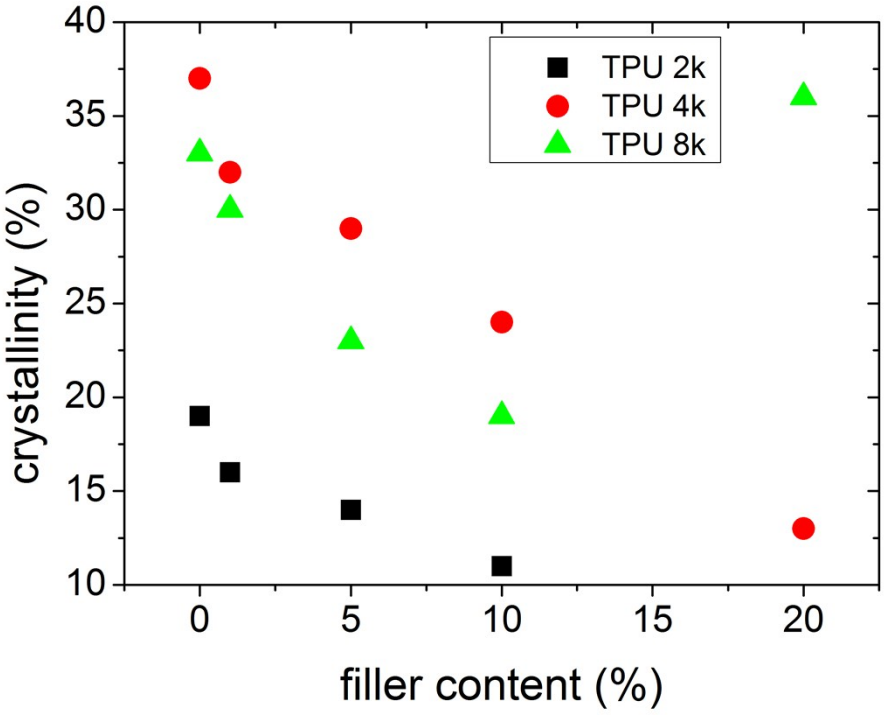

Supporting Figure 11 Crystallinity results by WAXS. The values are normalized to the soft segment fraction.

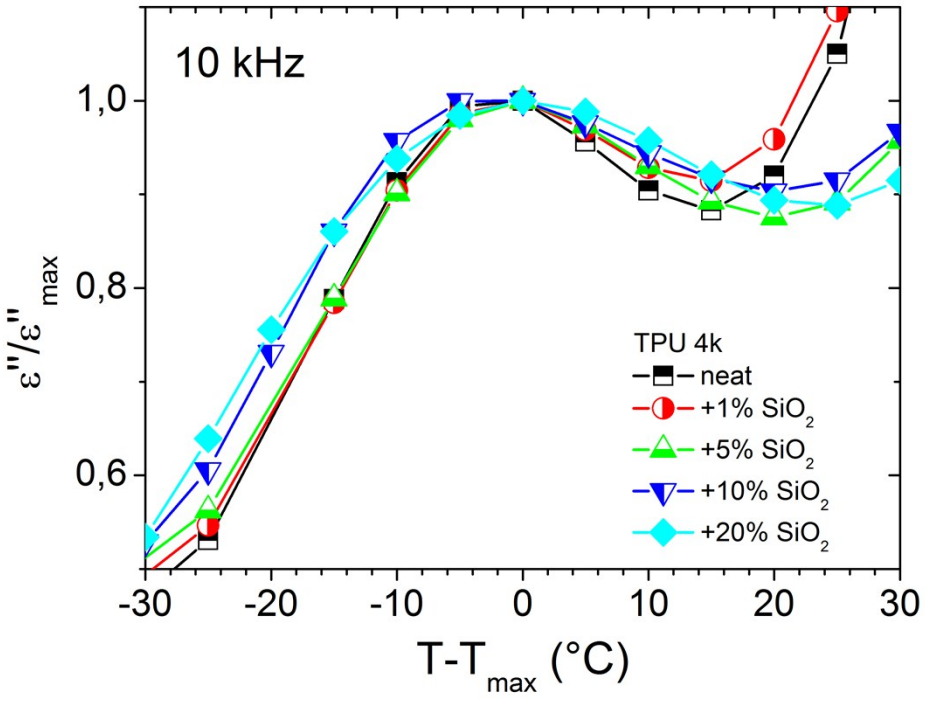

Supporting Figure 12 Comparative normalized DRS plots ($\varepsilon''/\varepsilon''_{max}$ vs $T-T_{max}$) at 10 kHz for the α-relaxation in the TPU 4k series in peak region. The curves have been translated in order for the peak maxima to coincide.

The scattering curves at low angles for the three matrices and the results of calculation for the interdomain distances can be bound in Supporting Figure 13.

Using Bragg's law $d = 2\pi / q_{max}$,[16] the interdomain distance of hard segments is estimated from the position of the peak.

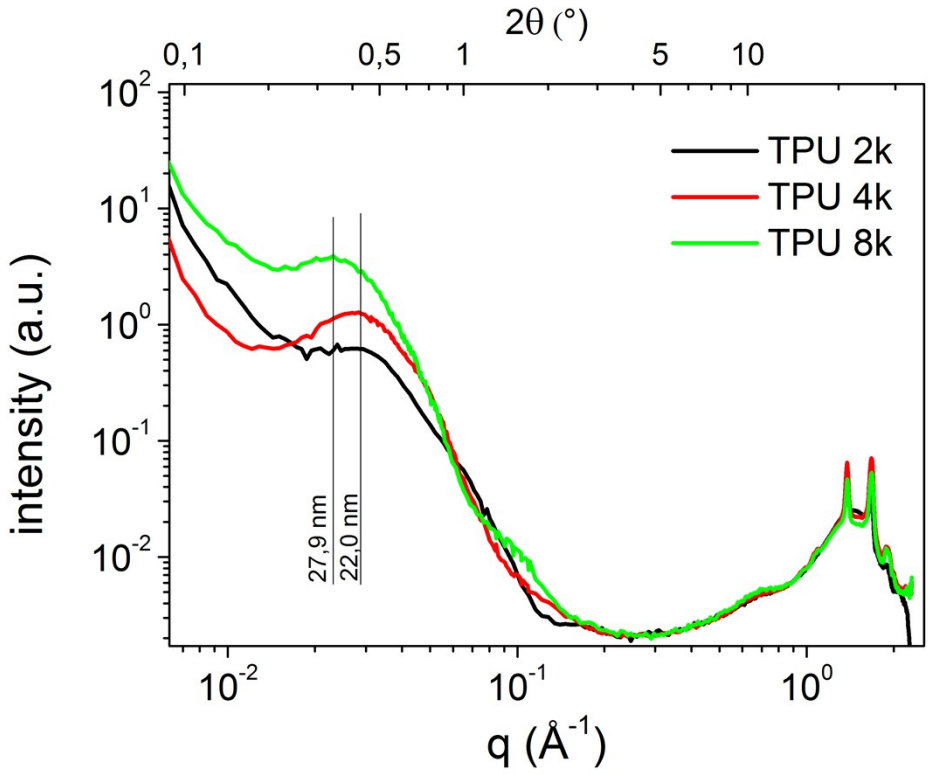

Supporting Figure 13 X-ray scattering curves normalized for sample thickness for the three neat matrices.

Supporting Figure 14 and Supporting Figure 12 show clearly that the α-relaxation becomes slower and broader, respectively, on addition of filler. This is an indication that the polymer bound at the interfaces with the filler is dielectrically not immobile, but displays slower dynamics resulting in a wider distribution of relaxation times.

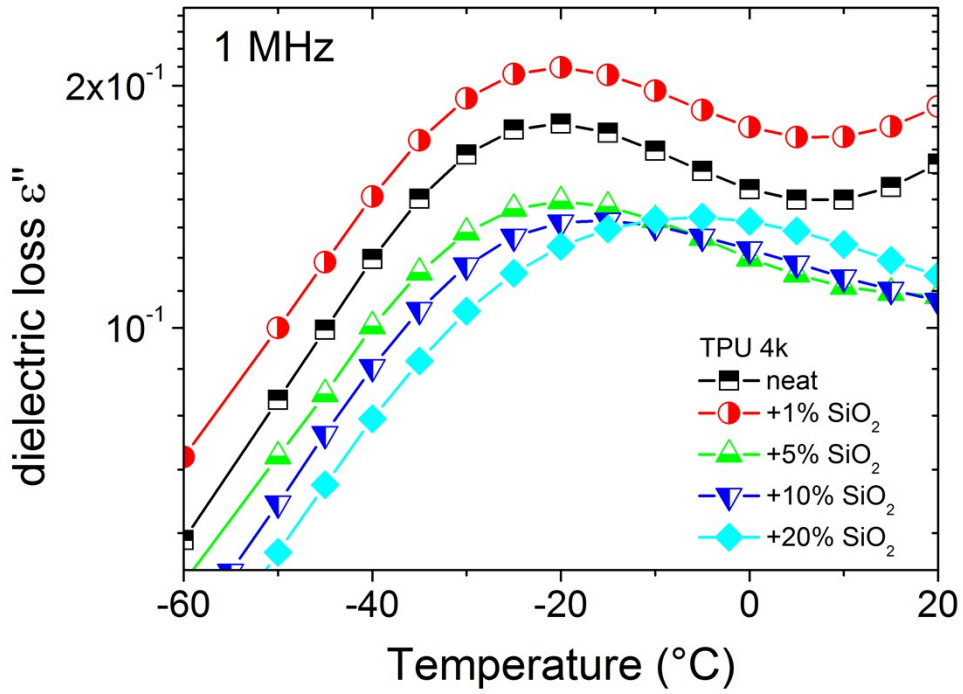

Supporting Figure 14 Isochronal diagrams of dielectric loss versus temperature at 1 MHz in the temperature range of the α-relaxation for the TPU 4k series. The experimental points are noted as dots and they are connected with lines so the eye can follow the pattern.

Supporting Figure 15 shows the Arrhenius plot for all relaxations measured in the matrix TPU 4k.

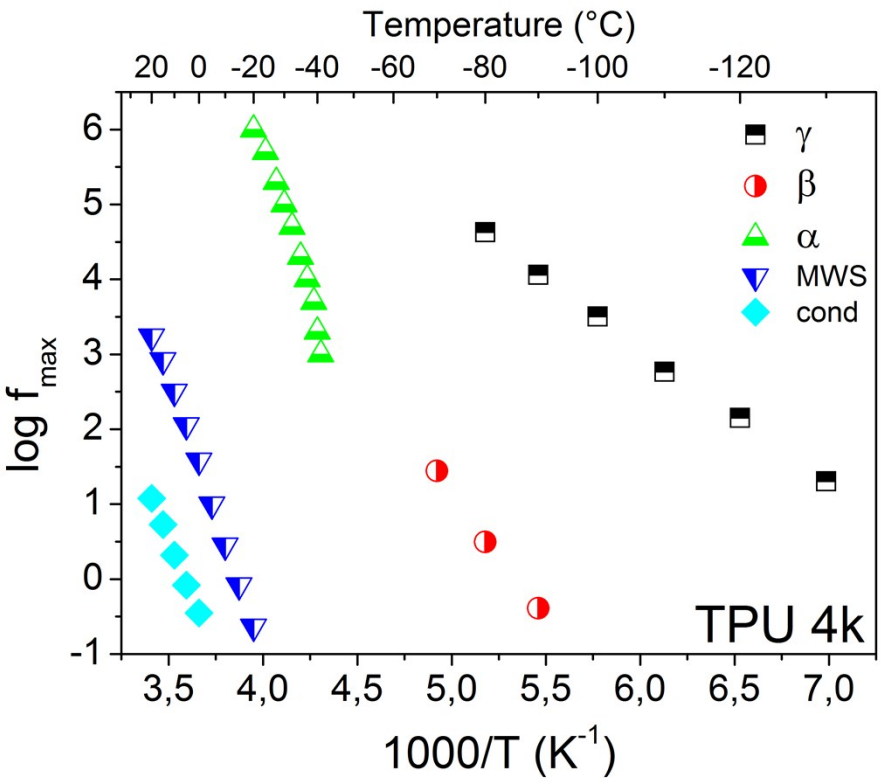

Supporting Figure 15 Arrhenius plot for the TPU 4k neat matrix where all the relaxations are presented

It is worth mentioning that the calculation of glass transition temperature using the raw data gives slightly lower values than those calculated by the derivative method. The derivative method computes the point where the slope of the raw data changes, whereas the commonly used half C_p extrapolation computes the midpoint of the transition. The midpoint and the point where the slope changes do not necessarily coincide, an example for that being shown in Supporting Figure 16.

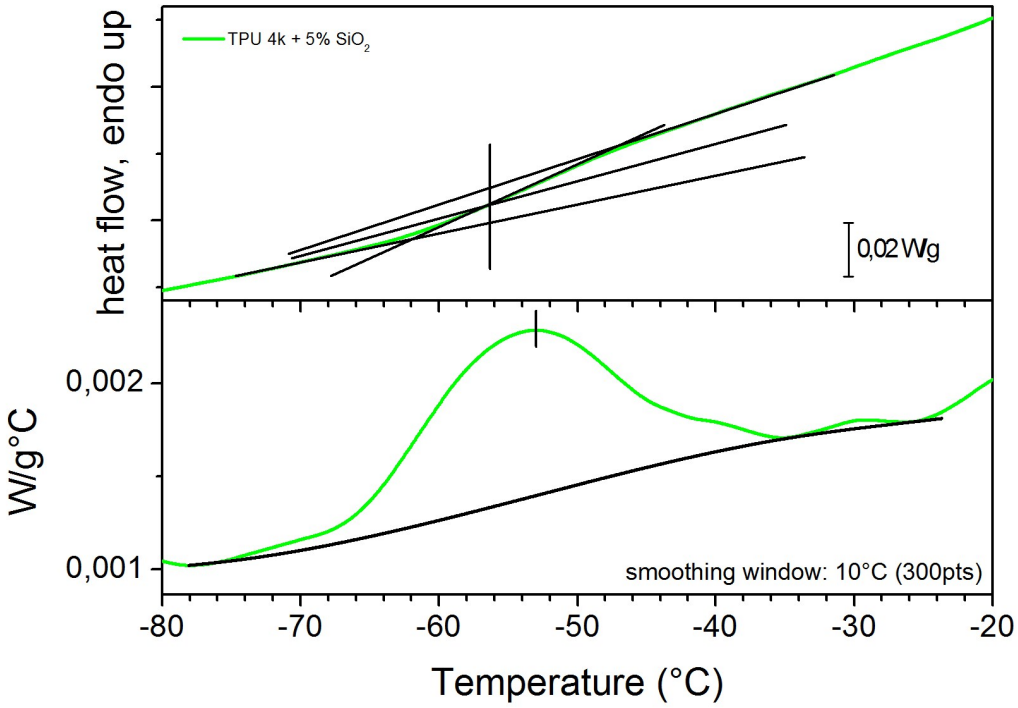

Supporting Figure 16 Example of the calculation for T_g and ΔC_p using the raw data curve (up) and the derivative curve (down).

A quick comment on reasons for $RAF_{crystal}$ to be completely immobile. One possible option is that the macromolecules around the crystals that consist the $RAF_{crystal}$ are partly stud inside the crystal: then the free part of the molecule is either completely rigid or has very long relaxation times that we cannot follow in our frequency range. Another possible option is that amorphous polymer is trapped in very small spaces between the crystal lamellas ore crystal defects, 1-2 nm, less than the cooperativity length of the relaxation,[2,17,18] and cannot display segmental dynamics.

References

1 S. Havriliak and S. Negami, *Polymer*, 1967, **8**, 161–210.

2 E.-J. Donth, *The Glass Transition: Relaxation Dynamics in Liquids and Disordered Materials*, Springer, 2001.

3 P. Klonos, A. Panagopoulou, L. Bokobza, A. Kyritsis, V. Peoglos and P. Pissis, *Polymer*, 2010, **51**, 5490–5499.

4 M. Wübbenhorst and J. van Turnhout, *J. Non. Cryst. Solids*, 2002, **305**, 50–58.

5 A. Kyritsis, G. Vikelis, P. Maroulas, P. Pissis, B. Milosheva, R. Kotsilkova, A. Toplijska, C. Silvestre and D. Duraccio, *J. Appl. Polym. Sci.*, 2011, **121**, 3613–3627.

6 U. W. Gedde, *Polymer Physics*, Chapman & Hall, London, 1995.

7 A. Kanapitsas, P. Pissis and A. Garcia Estrella, *Eur. Polym. J.*, 1999, **35**, 923–937.

8 K. N. Raftopoulos, B. Janowski, L. Apekis, P. Pissis and K. Pielichowski, *Polymer*, 2013, **54**, 2745–2754.

9 F. Garwe, A. Schonhals, H. Lockwenz, M. Beiner, K. Schroter and E. Donth, *Macromolecules*, 1996, **29**, 247–253.

10 S. Koutsoumpis, K. N. Raftopoulos, J. Pagacz, E. Hebda, C. M. Papadakis, K. Pielichowski and P. Pissis, *Macromolecules*, 2016, **49**, 6507–6517.

11 K. N. Raftopoulos, C. Pandis, L. Apekis, P. Pissis, B. Janowski, K. Pielichowski and J. Jaczewska, *Polymer*, 2010, **51**, 709–718.

12 G. Georgoussis, A. Kanapitsas, P. Pissis, Y. V Savelyev, V. Y. Veselov and E. G. Privalko, *Eur. Polym. J.*, 2000, **36**, 1113–1126.

13 E. Neagu, P. Pissis, L. Apekis and J. L. G. Ribelles, *J. Phys. D. Appl. Phys.*, 1997, **30**,

1551–1560.

14 D. Fragiadakis and P. Pissis, *J. Non. Cryst. Solids*, 2007, **353**, 4344–4352.

15 P. Klonos, P. Pissis, V. M. Gun'ko, a. Kyritsis, N. V. Guzenko, E. M. Pakhlov, V. I. Zarko, W. Janusz, J. Skubiszewska-Zieba and R. Leboda, *Colloids Surfaces A Physicochem. Eng. Asp.*, 2010, **360**, 220–231.

16 Y. Li, W. Kang, J. O. Stoffer and B. Chu, *Macromolecules*, 1994, **27**, 612–614.

17 J. Dobbertin, A. Hensei and C. Schick, *J. Therm. Anal. Calorim.*, 1996, **47**, 1027–1040.

18 Y. Termonia, *Polymer*, 2009, **50**, 1062–1066.